The Thermoelectric Properties of Mixed Crystals of $Mg_2Ge_xSi_{1-x}$

Richard J. LaBotz,[1] Donald R. Mason, and Daniel F. O'Kane[2]

The College of Engineering, The University of Michigan, Ann Arbor, Michigan

ABSTRACT

The purpose of this work was to determine the thermoelectric properties of the pseudobinary system Mg_2Si-Mg_2Ge. The compositions investigated were Mg_2Si, $Mg_2Ge_{0.2}Si_{0.8}$, $Mg_2Ge_{0.4}Si_{0.6}$, $Mg_2Ge_{0.6}Si_{0.4}$, $Mg_2Ge_{0.8}Si_{0.2}$, and Mg_2Ge. X-ray diffraction lattice parameter measurements and differential thermal analysis measurements established the existence of complete solid solubility between Mg_2Si and Mg_2Ge. Both the lattice parameter and liquidus temperature show almost linear variation with composition in this system. The melting temperature of Mg_2Si was found to be $1070° \pm 5°C$, while that of Mg_2Ge was found to be $1102° \pm 5°C$.

Electrical resistivity and Hall effect measurements indicated that at $300°K$ the electron Hall mobility in the mixed crystals is essentially the same as that of the pure compounds. Maximum values obtained were slightly above 300 cm^2/volt sec. The forbidden energy gap appeared to vary monotonically from about 0.78 electronvolt (ev) for Mg_2Si to about 0.70 ev for Mg_2Ge. Thermal conductivity measurements on the pseudobinary system showed that the lattice thermal conductivity of the solid solutions is substantially lower than that of either of the pure compounds at $300°K$. At this temperature the lattice thermal conductivity of $Mg_2Ge_{0.6}Si_{0.4}$ was found to be 0.0268 watt/cm $°K$. The maximum thermoelectric figure of merit which could be obtained with these materials is not as good as that of other materials now in use.

Lattice parameter determinations, differential thermal analysis measurements, and microscopic examinations at six different compositions in the system Mg_2Ge-Mg_2Si showed that there was complete solid solubility between Mg_2Si and Mg_2Ge; thermal conductivity, Seebeck coefficient, electrical conductivity, and Hall effect were measured on these samples, and all data were analyzed to correlate the results with theory.

No prior work has been reported in the literature on the Mg_2Ge-Mg_2Si mixed crystals, although previous investigators have made many measurements on Mg_2Ge and Mg_2Si. The electrical properties of single crystals of Mg_2Ge have been measured by Whitsett (1) and by Redin (2), while the electrical properties of polycrystalline samples of Mg_2Ge have been measured by Busch and Winkler (3). The electrical properties of single crystals of Mg_2Si have been investigated by Whitsett (1), by Morris (4), and by Ellickson and Nelson (5). The electrical properties of polycrystalline samples of Mg_2Si have been measured by Busch and Winkler (3).

Lattice parameter measurements have been performed on Mg_2Ge by Busch and Winkler (3), Klemm and Westlining (6), Brauer and Tiesler (7), Zintl and Kaiser (8), and Farrel (9). Similar measurements were performed on Mg_2Si by Owen and Preston (10), Klemm and Westlining (6), Busch and Winkler (3), and Farrel (9).

Melting temperature determinations were made on Mg_2Ge by Klemm and Westlining (6). The melting temperature of Mg_2Si has been measured by Vogel (11), by Klemm and Westling (6), and by Wohler and Schliephake (12). The thermal conductivities of Mg_2Ge and Mg_2Si have been measured in conjunction with this work and are reported in the previous paper (13).

The only mixed crystal system containing either Mg_2Ge or Mg_2Si that has been reported is the system Mg_2Ge-Mg_2Sn. The electrical properties and lattice parameter of mixed crystals of this system were measured by Busch and Winkler (14).

Experimental Results

The technique used to prepare the samples has been described in the previous paper (13). It was necessary to prepare 115 ingots before 13 satisfactory specimens of compositions Mg_2Si, $Mg_2Si_{0.8}Ge_{0.2}$, $Mg_2Si_{0.6}Ge_{0.4}$, $Mg_2Si_{0.4}Ge_{0.6}$, $Mg_2Si_{0.2}Ge_{0.8}$, and Mg_2Ge were obtained for measurements. The latter three compositions all tended to decompose in water or humid air, and these samples were stored in acetone to protect them.

The results of the x-ray lattice parameter measurements and the differential thermal analyses established the isomorphous nature of the pseudobinary system $Mg_2Ge_xSi_{1-x}$.

X-ray lattice parameter measurements.—The lattice parameter of each of the six different compositions tested was determined by use of x-ray powder diffraction techniques (15). The results of these measurements, shown in Fig. 1, indicate complete
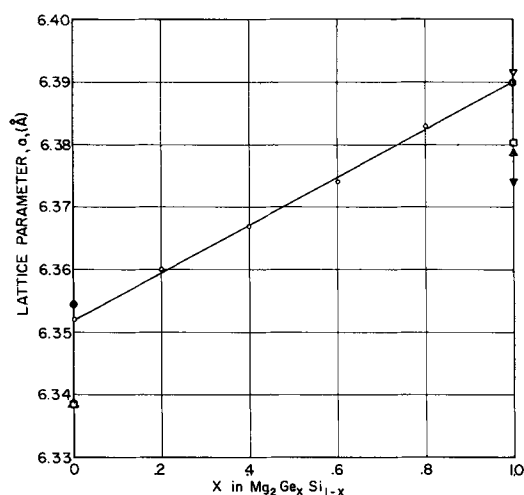
Fig. 1. Lattice parameter vs. composition for the system $Mg_2Ge_xSi_{(1-x)}$. Open circle, this work; solid circle, Farrel (9); open square, Klemm and Westlining (6); open triangle, Busch and Winkler (3); inverted open triangle, Owen and Preston (10); solid triangle, Zintl and Kaiser (8); inverted solid triangle, Brauer and Tiesler (7).

Fig. 2. Liquidus temperature vs. composition for the system $Mg_2Ge_xSi_{(1-x)}$. X. This work; open circle, Klemm and Westlining (6); open triangle, Vogel (11); open square, Wohler and Schiephake (12).

Fig. 3. Mg-Ge-Si ternary phase diagram

solid solubility between the compounds Mg_2Si and Mg_2Ge, the slight variation in results being due to experimental error.

The measured lattice parameter of the mixed crystals varies linearly with the composition, showing unusually good agreement with Vegard's law. This type of behavior can be expected in substitutional solid solutions with atoms of similar size and electronic structure (15). Similar results were obtained by Busch and Winkler (14) in their work on the pseudobinary system Mg_2Ge-Mg_2Sn.

Differential thermal analysis measurements.— Differential thermal analysis measurements were made on each of the six compositions in order to construct the pseudobinary phase diagram. The samples were held in a boron nitride crucible using an empty boron nitride crucible as a reference. The sample crucible and the reference crucible were heated inside a low carbon steel block which in turn was contained in a zirconia tube that was closed at one end. The other end of the zirconia tube was fitted with an "O" ring seal so that the tube could be evacuated and backfilled with argon in order to suppress the vaporization of magnesium as much as possible. Measurements were made under about 1½ atm. of argon. Samples were heated in a Kanthal resistance furnace which had an automatic control to provide a substantially linear heating rate of about 3°K/min. The results of these measurements and those of previous investigators are plotted in Fig. 2.

Since there was a fair amount of supercooling and a loss of magnesium vapor from the molten material, only heating curves were used for the phase diagram determination, and it was not possible to determine the solidus temperature accurately.

No transitions other than the melting phenomenon were observed in the heating curves, but the cooling curves showed a very slight transition at the magnesium-deficient eutectic temperature
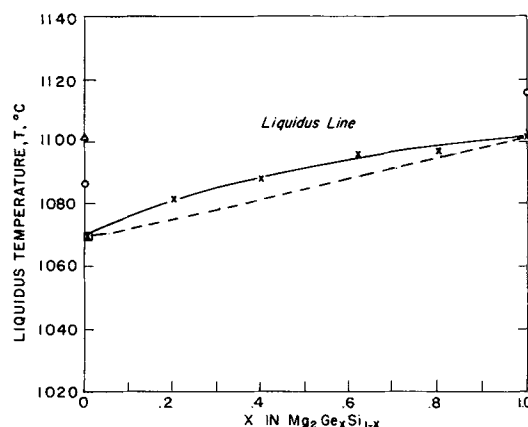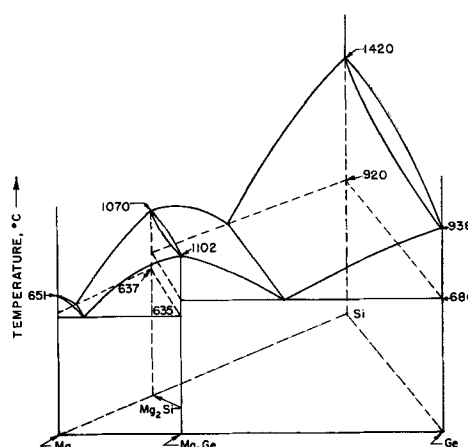
whenever magnesium had been lost at elevated temperatures.

These results also indicate that Mg_2Ge and Mg_2Si form an isomorphous system. A complete Mg-Ge-Si ternary phase diagram is given in Fig. 3.

Electrical measurements.—Electrical resistivity and Hall effect measurements are carried out using conventional direct current techniques (16). The direct current supplied by a Lambda Model 65M power supply was filtered to reduce ripple by use of an 8.5 h choke and a 40 μf capacitor. Resistors in series with the sample were used to obtain the desired current level. Switches were available for reversing the polarity of the current, the Hall probes, and the electrical resistivity probes. The potential readings were taken with a L&N K-2 potentiometer.

The magnetic field used in the Hall effect measurements was obtained by use of a 2100 gauss permanent magnet. This magnet had a pole face diameter of 2½ in. and a 2¾ in. gap. To facilitate reversing the magnetic field the magnet was mounted on a large roller bearing, and the magnet could be rotated exactly 180° without moving the sample.

Electrical contacts were made to the test specimens by leaf springs made from rhodium-plated beryllium copper. These leaf springs were fastened to small copper blocks which in turn are mounted

on a lavite platform. The rectangular specimen was held in place by pressure contacts which also served as current leads. The sample holder was patterned after the design published by Brooker, Clay, and Young (17). The sample holder is mounted with stainless steel screws. Directly over the sample holder are two molybdenum tubes containing 30 gauge chromel-alumel thermocouples, which were used to check the temperature gradient along the sample.

A 2½ in. long copper shield is placed over the sample holder while a solid copper rod with a heater mounted on it is connected to the lower end of this shield. The heater is made on a threaded piece of lavite which is wrapped with 28 gauge chromel heating wire. The large mass of solid copper rod is used to damp out temperature fluctuations.

Connected to the top end of the copper shield is a ½ in. copper tube with a copper spacer and a lavite heater similar to the lower heater. A lavite spacer prevents thermal conduction up the copper tube. A Vycor tube encloses the sample and supporting apparatus and is wrapped with Pyrex wool to reduce heat losses. The open end of the Vycor tube is sealed by means of "O" ring seals to a mounting coupling. The ½ in. copper tube passes through this coupling by means of seals which allow the vertical positioning of the sample directly between the poles of the magnet. An outlet from the coupling leads to a pressure gauge, a vacuum system, and the hydrogen supply. The samples were measured under a hydrogen atmosphere. Oxygen and water vapor are removed from the hydrogen by passing it through a "Deoxo" catalyst and then through molecular sieves.

The thermal conductivities and Seebeck coefficients were measured with the apparatus described in the preceding paper (13).

The results of electrical resistivity measurements on the six different compositions are plotted in Fig. 4. The onset of intrinsic behavior follows no consistent pattern since the impurity concentration was an uncontrolled variable in the investigation.

The measurements of the Seebeck coefficient are presented in Fig. 5. The Hall coefficient data were sufficiently extensive in the intrinsic region of only $Mg_2Ge_{0.4}Si_{0.6}$ and Mg_2Ge to permit an evaluation of the energy gap. Plots of log $|R_HT^{3/2}|$ against reciprocal absolute temperature are shown in Fig. 6, and the derived energy gaps are also tabulated in Table
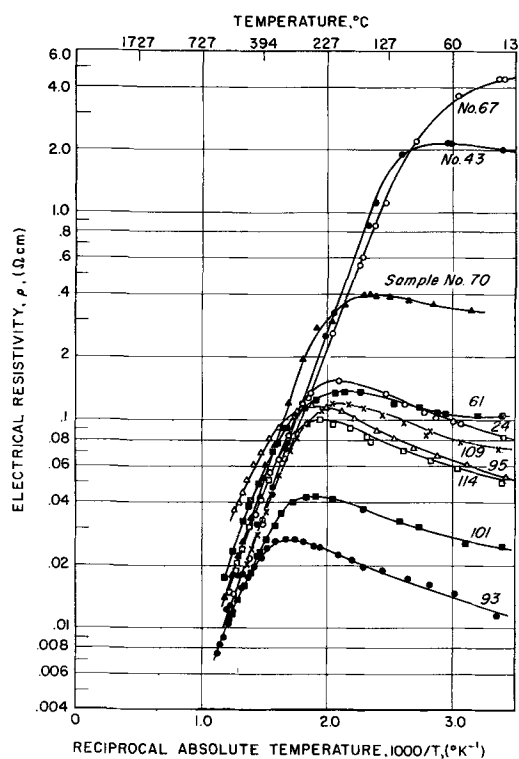
Fig. 5. Seebeck coefficient vs. absolute temperature
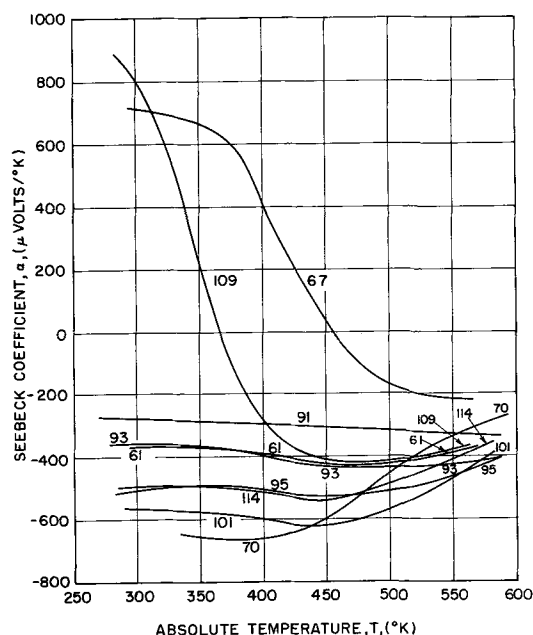
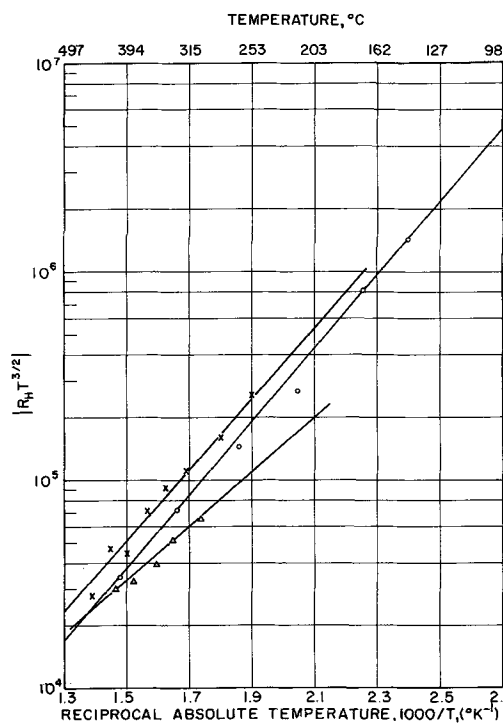**Fig. 4. Logarithm of electrical resistivity vs. reciprocal absolute temperature.**

Fig. 6. Logarithm of $|R_HT^{3/2}|$ vs. reciprocal absolute temperature

Table I. Summary of results obtained from measurements on the system $Mg_2Ge_xSi_{1-x}$

	E_{g_0}, ev ρ vs. 1/T	E_{g_0}, ev $\lvert R_H T^{3/2}\rvert$	Extrinsic mobility $\mu_H = \mu_0 T^\gamma$ cm²/v sec	Intrinsic mobility $\lvert R_H/\rho\rvert =$ $\lvert R_H/\rho\rvert_0 T^\gamma$ cm²/v sec	$\lambda_{300°K}$, w/cm °K	Sat'n impurity conc'n $\lvert N_D - N_A\rvert$, carriers/cm³	Z_{max}, °K⁻¹	m_n^*	Resistivity, $\rho_{300°K}$, ohm-cm	Seebeck Coef. $\alpha_{300°K}$, μv/°K
Mg_2Si										
No. 95	[~0.72]		[160]$(T/300)^{-1.7}$	[420]$(T/300)^{-3.1}$		9×10^{17}	3.3×10^{-4}	$1.0m_0$	0.06(n)	−505
No. 24	[~0.65*]		350*			2.6×10^{17}			0.09(n)*	
No. 91					0.0792					−275
$Mg_2Ge_{0.2}Si_{0.8}$										
No. 93	0.79		310$(T/300)^{-1.5}$			2×10^{18}	6.7×10^{-4}	$0.51m_0$	0.0114(n)	−370
No. 115					0.0355					
$Mg_2Ge_{0.4}Si_{0.6}$										
No. 70	0.75	0.74	[187]$(T/300)^{[-1.0]}$	[350]$(T/300)^{-2.4}$		1.4×10^{17}	[2.6×10^{-3}]	[$0.15m_0$]	0.035(n)	−650
No. 101	[0.72]	[0.58]	273$(T/300)^{-1.4}$	640$(T/300)^{-2.6}$	0.0289	1.3×10^{18}		$0.58m_0$	0.026(n)	−570
$Mg_2Ge_{0.6}Si_{0.4}$										
No. 61	[0.70]		[70]	[160]$(T/300)^{[-2.1]}$		1×10^{18}	9.4×10^{-4}		0.11(n)	−375
No. 114	0.75		280$(T/300)^{-1.6}$	530$(T/300)^{-2.5}$	0.0289	5.8×10^{17}		$0.85m_0$	0.051(n)	−500
$Mg_2Ge_{0.8}Si_{0.2}$										
No. 109	0.71*	0.72*	310*$(300/T)^{-1.4*}$	620*$(T/300)^{-2.7*}$	0.0405*	3.5×10^{17}			0.07(n)	+800(p)*
No. 108			342*			2.9×10^{17}				
Mg_2Ge			Sample going from p to n over range of Hall measurements.							
No. 43	0.70					1.3×10^{17}			2.0(p)	
No. 67	[0.71]	0.70	[175]$(T/300)^{[-1.2]}$	[360]$(T/300)^{-2.4}$	0.0628	9.5×10^{15}			4.0(n)	+710(p)
Average			300$(T/300)^{-1.5}$	600$(T/300)^{-2.5}$						

* Single crystal data.
Values in brackets are doubtful.

I. The saturation impurity carrier concentration in the extrinsic region as determined from the Hall effect measurements (16) is also tabulated in Table I for each sample that was measured. The impurity concentration varied erratically from 10^{16} to 10^{18} carriers/cm³.

The Hall mobility factor, R_H/ρ, is plotted against absolute temperature on logarithmic coordinates in Fig 7. The extrinsic Hall mobility at 300°K is given as a function of composition in Table I. The amount of variation from one composition to the next is no greater than the variation observed from one sample to another of the same composition. The maximum mobilities observed for the mixed crystals of $Mg_2Ge_{0.2}Si_{0.8}$, $Mg_2Ge_{0.4}Si_{0.6}$, and $Mg_2Ge_{0.6}Si_{0.4}$ are lower than those observed in Mg_2Si and $Mg_2Ge_{0.8}Si_{0.2}$. It appears as though this reduction in 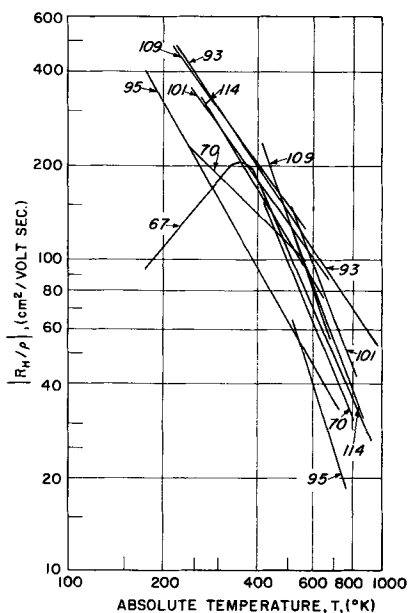the maximum observed mobility is not due to the formation of mixed crystals because relatively high mobilities were observed for the mixed crystal samples of $Mg_2Ge_{0.8}Si_{0.2}$. A more satisfactory explanation is that the mobility difference is associated with the form of the material being measured. The higher mobilities for Mg_2Si and $Mg_2Ge_{0.8}Si_{0.2}$ were measured in single crystals, whereas the slightly lower maximum mobilities measured in the other mixed crystals were measured in polycrystalline specimens. If all mobility measurements had been made on single crystals it is quite likely that no decrease in the maximum mobility would have been observed, and that the average mobility would be slightly greater than 300 cm²/volt sec at 300°K. The average temperature dependence of the mobility (−3/2 power) indicates that lattice scattering is the predominant scattering mechanism.

The high mobilities reported by Winkler (3) for polycrystalline Mg_2Si (370 cm²/volt sec) and Mg_2Ge (530 cm²/volt sec) were obtained by extrapolating high-temperature data to obtain a room temperature value, and are actually intrinsic mobility values extrapolated to room temperature rather than measured extrinsic mobilities.

When a similar extrapolation is applied to the data obtained in this investigation, room temperature mobilities which are two to three times higher than those actually measured are obtained, and the results of this extrapolation are also tabulated in Table I. The average temperature dependence of the intrinsic Hall mobility (−5/2 power) indicates that hole-electron scattering is apparently the predominant scattering mechanism.

Once the temperature dependence of the mobility is known (−γ), a plot of log ($\rho T^{3/2-\gamma}$) against reciprocal absolute temperature can be made. The straight line in the intrinsic conductivity region then has a slope of $E_{g_0}/4.6k$, and the energy gaps for these materials were determined in this way. The value of energy gap from this investigation for Mg_2Si is not very precise, and Morris' value of

Fig. 7. Logarithm of $\lvert R_H/\rho\rvert$ vs. logarithm of absolute temperature

0.78 ev[4] is undoubtedly more correct. From Table I then it can be noticed that the energy gap decreases from a value of about 0.78 ev for Mg_2Si to about 0.70 ev for Mg_2Ge. On the basis of this data it is difficult to state whether the energy gap varies linearly with composition or not. Busch and Winkler (14) in their work on the Mg_2Ge-Mg_2Sn solid solution found a nonlinear variation of energy gap with composition. However, it should be pointed out that the energy gap in the Mg_2Ge-Mg_2Sn system changes from 0.70 ev for Mg_2Ge to 0.36 ev for Mg_2Sn, which is considerably greater than that experienced in going from Mg_2Si to Mg_2Ge.

The Seebeck coefficient data show the temperature at which intrinsic behavior commences in each sample (18). Also in conjunction with the saturation impurity concentration, the Seebeck coefficient can be used to determine the effective mass of the electrons. The results are also tabulated in Table I.

Thermal Conductivity

The thermal conductivity of a semiconductor at moderate temperatures is generally considered to be the sum of the lattice and charge carrier components. For nondegenerate materials these components are essentially independent of each other.

The charge carrier component is made up of contributions from various mechanisms such as the normal thermal diffusion of charge carriers as described by the Wiedeman-Franz relationship, ambipolar diffusion, and diffusion of excitons. The methods of calculating these contributions from measured electrical and thermal conductivity data are given in the literature (19).

The lattice thermal conductivity is the result of energy transport by phonons. The magnitude of the lattice thermal conductivity is a function of the amount of phonon scattering which takes place within the lattice. The nature of the scattering which exists in the lattice can be determined to a large extent by an examination of the temperature dependence of the lattice thermal conductivity, as various scattering mechanisms have different temperature dependencies (20).

The substitutional solid solutions examined in this investigation would be expected to have a strong point defect scattering due to the large mass difference between the silicon and germanium. As pointed out by Klemens (21)

$$\lambda \propto T^{-1/2} \epsilon^{-1/2}$$

for temperatures above the Debye temperature. The term ϵ accounts for the concentration of point defects and is given by

$$\epsilon = \sum_j C_j (M_j - M)^2 / M^2 \qquad [1]$$

$$M = \sum_j C_j M_j \qquad [2]$$

where C_j and M_j are the concentration and mass of atoms of type j. This is in contrast to the

$$\lambda \propto T^{-1} \qquad [3]$$

which would be expected for the pure compounds.

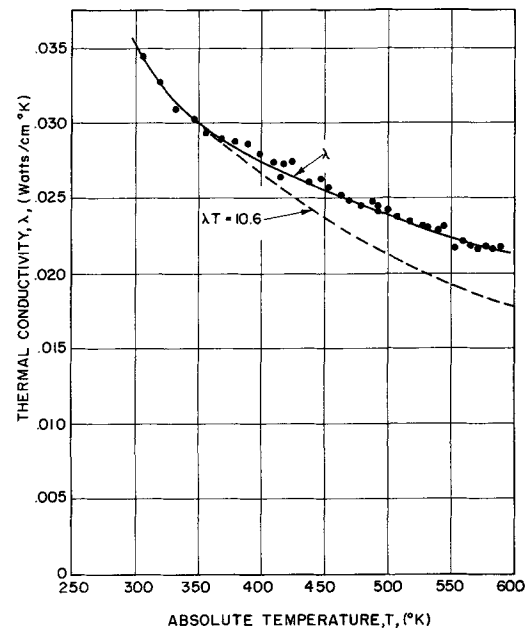*Thermal conductivity of* $Mg_2Ge_{0.2}Si_{0.8}$.—The thermal conductivity of $Mg_2Ge_{0.2}Si_{0.8}$ was measured on

Fig. 8. Thermal conductivity for $Mg_2Ge_{0.2}Si_{0.8}$, sample No. 115, *vs.* absolute temperature.

sample No. 115. However, due to a lack of reproducibility in the electrical measurements made on this sample there is some question as to the quality of the ingot. For this reason the results are presented in Fig. 8 without comment simply for the sake of completeness.

Thermal conductivity of $Mg_2Ge_{0.4}Si_{0.6}$—The thermal conductivity of $Mg_2Ge_{0.4}Si_{0.6}$ was measured on sample No. 101. This sample was large grained and contained no visible eutectic. It was 1.67 cm long and had a cross-sectional area of 2.30 cm².

In Fig. 9 the experimentally determined values of thermal conductivity and the calculated values of the electron component are given as functions of temperature. The quantity $(\lambda_{th} - \lambda_{el})$ is not plotted as this value is very close to λ_{th}.

By matching curves at 300°K the relationship $\lambda_{lattice} = 0.512T^{-1/2}$ watts/cm °K was determined. The experimental values follow this relationship
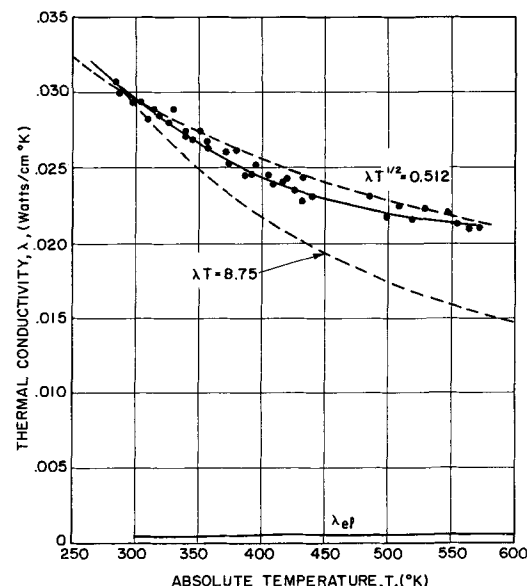

Fig. 9. Thermal conductivity for $Mg_2Ge_{0.4}Si_{0.6}$, sample No. 101, *vs.* absolute temperature.
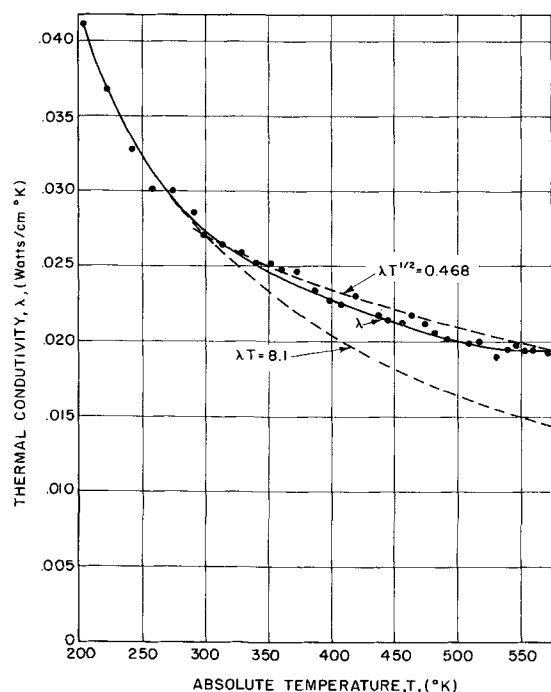
Fig. 10. Thermal conductivity for Mg₂Ge₀.₆Si₀.₄, sample No. 114, vs. absolute temperature.

Fig. 11. Thermal conductivity for Mg₂Ge₀.₈Si₀.₂, sample No. 109, vs. absolute temperature.

rather well, indicating that point defect scattering predominates.

Thermal conductivity of $Mg_2Ge_{0.6}Si_{0.4}$.—The thermal conductivity of $Mg_2Ge_{0.6}Si_{0.4}$ was measured on sample No. 114. This sample was large grained and free of eutectic, had a cross-sectional area of 1.65 cm², and was 1.37 cm long.

A plot of the experimental values of thermal conductivity as a function of temperature for this sample is given in Fig. 10. The electron component of thermal conductivity for this sample is negligible. Thus lattice thermal conductivity is essentially equal to the measured values.

Due to a rather unusual set of experimental circumstances it was possible to make thermal conductivity measurements from 200°K. The results are rather interesting.

From 200°K to 300°K the lattice thermal conductivity is proportional to T^{-1}, while above 300°K the lattice thermal conductivity is proportional to $T^{-1/2}$. Thus above about 300°K $\lambda = 0.468T^{-1/2}$ watts/cm °K, while from 200°K to 300°K $\lambda = 8.10T$ watts/cm °K. Although the behavior above 300°K is explainable in terms of the mass difference point defect scattering, the reason for the sharp transition at 300°K is not apparent.

Thermal conductivity of $Mg_2Ge_{0.8}Si_{0.2}$.—The thermal conductivity of $Mg_2Ge_{0.8}Si_{0.2}$ was measured on sample No. 109. This sample appeared to be a single crystal. As all the better ingots of this composition were composed of a number of relatively large single crystals which were very weakly bound together, it was decided to use the largest crystal available for making the thermal conductivity specimen. For this reason, this specimen was the smallest one which was tested in the whole sequence. It had a cross-sectional area of 0.87 cm². The small cross section resulted in very low heating rates being used in the thermal conductivity meas-
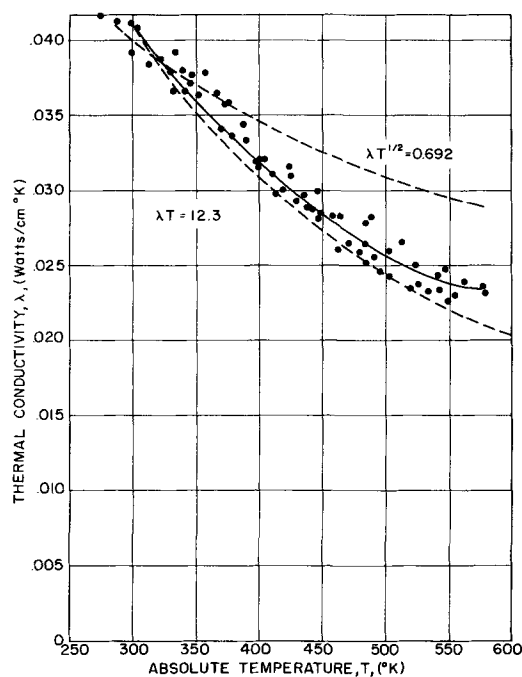
urements. These low heating rates made heating rate determinations difficult, producing a large amount of scatter in the final results.

The experimentally determined thermal conductivity is given as a function of temperature in Fig. 11. Due to the fact this was a single crystal its thermal conductivity would not necessarily correlate very well with that of the other samples, as its properties were nonisotropic.

The exact temperature dependence of the thermal conductivity is difficult to determine due to the scatter of the experimental data. However, it does lie between the $T^{-1/2}$ and T^{-1} temperature dependence lines. This suggests that possibly the thermal resistance could be a combination of point defect and normal Umklapp scattering.

Variation of lattice thermal conductivity with composition.—The variation of lattice thermal conductivity with composition and temperature is shown in Fig. 12. As just pointed out the values for $Mg_2Ge_{0.8}Si_{0.2}$ do not correlate very well with the other samples due to its nonisotropic nature.

The temperature-composition variation is not in good agreement with the expression given by Klemens. According to this expression the ratio of the conductivity from one composition to the next should be the same at any given temperature. However, this is not the case with the experimental data. As can be seen from Fig. 12 the differences in thermal conductivity from one composition to the next become significantly smaller as the temperature is raised. This would seem to indicate some sort of saturation effect in the phonon scattering at elevated temperatures as has been suggested by Ioffe (22).

Thermoelectric Figure of Merit

The final property which will be considered is the maximum thermoelectric figure of merit, Z_{max}, by the correlations presented by Simon (23). This
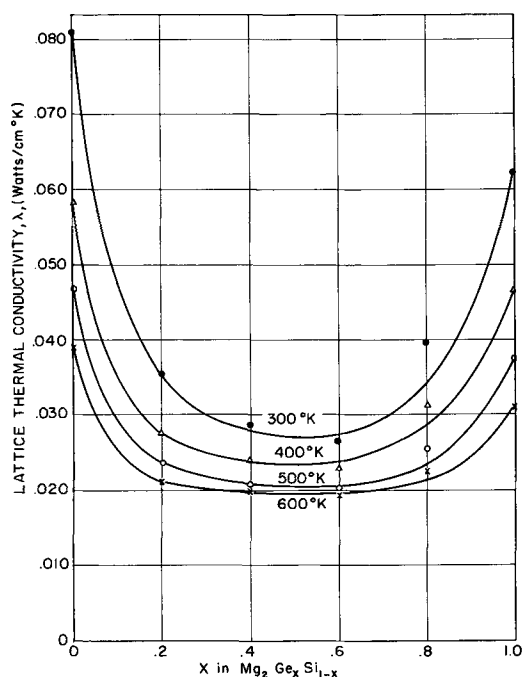
Fig. 12. Lattice thermal conductivity as a function of composition and temperature in the system $Mg_2Ge_xSi_{(1-x)}$.

quantity is also given in Table I for the four materials for which sufficient correlatable data are available. The variation in the maximum thermoelectric figure of merit should be proportional to the variation in the ratio μ_n/λ_{ph}. In going from Mg_2Si to $Mg_2Ge_{0.4}Si_{0.6}$ and $Mg_2Ge_{0.6}Si_{0.4}$ the ratio μ_n/λ_{ph} increases by a factor of about 2.4. Due to the nearly identical lattice thermal conductivity and electron mobility for $Mg_2Ge_{0.4}Si_{0.6}$, sample No. 101, and for $Mg_2Ge_{0.6}Si_{0.4}$, sample No. 114, it would be expected that these two samples would have almost identical values of Z_{max}. However, the optimized thermoelectric figure of merit increases by a factor of about 8.0 in going from Mg_2Si to $Mg_2Ge_{0.4}Si_{0.6}$ while it increases by a factor of 2.8 in going from Mg_2Si to $Mg_2Ge_{0.6}Si_{0.4}$. This indicates the value of Z_{max} for $Mg_2Ge_{0.6}Si_{0.4}$ is probably correct while that for $Mg_2Ge_{0.4}Si_{0.6}$ is probably too large by a factor of about 3.

As the value of Z_{max} is calculated on the basis of the extrinsic properties of the material, a difference in impurity carrier concentration between the specimens used to measure electrical resistivity and thermal conductivity could give rise to this discrepancy. In this case the electrical specimen should have a higher impurity level than the thermal conductivity specimen. It should be noted that such a difference in impurity levels would not have any effect on the intrinsic properties of the material.

Since the value of Z_{max} for the mixed crystals is considerably higher than that for Mg_2Si, the mixed crystals would be much better as thermoelectric materials than the pure compound if all the materials had the optimum impurity levels. Even under these optimized conditions, however, the mixed crystals would have a thermoelectric figure of merit somewhat lower than that of materials now in use.

Effects of nonstoichiometric specimens.—Since six of the samples on which measurements were made were either slightly nonstoichiometric or were taken from ingots which were nonstoichiometric as determined by microscopic examination, the effects of nonstoichiometry should be examined. Three of these samples were slightly silicon-rich, while the other three may have contained a trace of excess magnesium.

Morris (4) and Redin (2) in their work at Iowa State University found that an excess of silicon or an excess of germanium in an ingot does not affect the electrical properties of the Mg_2Si or the Mg_2Ge taken from the ingot. Morris in his work on single crystals of Mg_2Si took his single crystals from ingots containing large amounts of excess silicon. Redin obtained his single crystals of Mg_2Ge from ingots containing up to 66% of the germanium-rich eutectic. The low impurity carrier concentrations found in these investigations seem to indicate that neither the excess silicon nor the excess germanium enter the lattice as donors or acceptors. The data of Morris and Redin say nothing about the solubility of magnesium in either Mg_2Si or Mg_2Ge.

The electrical properties of polycrystalline samples of both stoichiometric and nonstoichiometric Mg_2Si and Mg_2Ge have been measured by Winkler (3). His measurements were made on Mg_2Si, Mg_2Ge, $Mg_2Si + 2\%$ Si, $Mg_2Si + 2\%$ Mg, $Mg_2Ge + 1\%Ge$, and $Mg_2Ge + 0.5\%$ Mg. Due to the extremely low limits of solubility found by Morris and Redin it must be concluded that the excess silicon and germanium in Winkler's samples showed up as eutectic inclusions in the grain boundaries.

Winkler's silicon-rich sample of Mg_2Si has an impurity carrier concentration only 15% higher than that of the pure Mg_2Si in the extrinsic region, while the Hall mobilities of the pure and the silicon-rich Mg_2Si are essentially identical. Although the silicon-rich specimen has a lower extrinsic resistivity due to its higher carrier concentration, it has identical properties with the pure material in the intrinsic region.

The magnesium-rich sample of Mg_2Si has an impurity carrier concentration approximately 40% higher than that of the pure sample. This indicates the solubility of magnesium in Mg_2Si is very slight, and that the excess magnesium probably shows up as eutectic inclusions in the grain boundaries. In the extrinsic region the mobility of magnesium-rich material is about 30% higher than that of the pure materials. Again in the intrinsic region the pure and impure material approach the same behavior.

The magnesium-rich sample of Mg_2Ge does not follow completely the trend set by the corresponding Mg_2Si sample. Although the impurity carrier concentration in the extrinsic region is about 25% higher than that of the pure Mg_2Ge, the electron Hall mobility is 10% lower than that of the pure material. The two samples again behave similarly in the intrinsic region.

Winkler found that the germanium-rich Mg_2Ge had an impurity carrier concentration which was

twice as high as that of the pure Mg_2Ge while the charge carrier mobility was 10% higher than that of the pure Mg_2Ge. None of the samples tested in this investigation had an excess of germanium.

Winkler made Seebeck coefficient measurements on only two samples of Mg_2Si the pure material and the silicon-rich sample. The impure sample had a value 5-10% lower than the pure material. This is better agreement than Winkler found between his pure samples of Mg_2Ge.

A few conclusions can be drawn from Winkler's data for samples containing eutectic inclusions. The presence of small eutectic inclusions of either silicon or magnesium does not affect the electrical properties in the intrinsic region. In the extrinsic region the excess magnesium and the excess silicon seem to cause a slight increase in the impurity carrier concentration. However, as the impurity carrier concentrations normally vary by an order of magnitude from one stoichiometric melt to another this change does not seem particularly significant. The excess silicon did not seem to have any effect on the charge carrier mobility, while the excess magnesium increased the mobility a slight amount in one case and decreased it a slight amount in another. In view of this it is possible that very small magnesium-rich eutectic inclusions do not materially affect the mobility and that the changes in mobility which were observed represent normal variations from one sample to the next.

The results of this investigation are in fairly good agreement with those of Winkler for the effects of nonstoichiometry. An excess of silicon did not seem to have any effect on the saturation impurity carrier concentration, although it did appear to produce a reduction in charge carrier mobility. The excess magnesium appeared to raise the saturation impurity carrier concentration to about 10^{18} electrons/cm^3, indicating a solubility of magnesium in the lattice of about 1 part per 100,000. The excess magnesium had no noticeable effect on the charge carrier mobility. The intrinsic properties of the material were not affected by the presence of either the excess silicon or the excess magnesium.

The thermal conductivity specimens measured in this investigation were either of stoichiometric composition or contained only a trace (0.01%) of excess magnesium. An analysis of the thermal conductivity data did not indicate any contribution to the thermal conductivity which could be attributed to the trace of magnesium.

Acknowledgments

REFERENCES

1. C. R. Whitsett, "Electrical Properties of Magnesium Germanide and Magnesium Silicide," Ph.D. Thesis, Iowa State College, Ames, Iowa, as quoted by Morris (4) and Redin (2) (1955).
2. a. R. D. Redin, "Semiconducting Properties of Mg_2Ge Single Crystals," Ph.D. Thesis, Iowa State University, University Microfilms, Inc., Ann Arbor, Mich. (1957).
   b. R. D. Redin, R. G. Morris, and G. C. Danielson, *Phys. Rev.*, **109**, 1916 (1958).
3. a. G. Busch and U. Winkler, *Physica*, **20**, 1067 (1954).
   b. U. Winkler, *Helv. Phys. Acta*, **28**, 633 (1955).
4. a. R. G. Morris, "Semiconducting Properties of Mg_2Si Single Crystals," Ph.D. Thesis, Iowa State University, University Microfilms, Inc., Ann Arbor, Mich. (1957).
   b. R. G. Morris, R. D. Redin, and G. C. Danielson, *Phys. Rev.*, **109**, 1909 (1958).
5. R. T. Ellickson and J. T. Nelson, "Semiconducting Properties of Intermetallic Compounds," Fifth Quarterly Progress Report, Department of Physics, University of Oregon, Eugene, Ore. as quoted by Morris (4).
6. W. Klemm and H. Westlining, *Z. anorg. Chem.*, **245**, 364 (1941).
7. V. G. Brauer and J. Tiesler, *Z. anorg. Chem.*, **262**, 319 (1950).
8. E. Zintl and H. Kaiser, *ibid.*, **211**, 125 (1933).
9. P. Farrel, "Lattice Parameter of Mg_2Si and Mg_2Ge," as quoted by Redin (2) and Morris (4).
10. E. A. Owen and G. D. Preston, *Proc. Phys. Soc.*, **36**, 341 (1924).
11. R. Vogel, *Z. anorg. Chem.*, **61**, 46 (1909).
12. L. Wohler and O. Schliephake, *ibid.*, **151**, 11 (1926).
13. R. J. LaBotz and D. R. Mason, *This Journal*, **110**, 121 (1963).
14. G. Busch and U. Winkler, *Helv. Phys. Acta*, **26**, 578 (1953).
15. C. Barrett, "The Structure of Metals," McGraw-Hill Book Co., New York (1952).
16. O. Lindberg, *Proc. I.R.E.*, **40**, 1414 (1952).
17. A. Brooker, R. Clay, and A. Young, *J. Sci. Inst.*, **34**, 512 (1957).
18. A. F. Ioffe, "Semiconductor Thermoelements and Thermoelectric Cooling," Infosearch, Ltd., London (1957).
19. A. F. Ioffe, "Physics of Semiconductors," Academic Press, New York (1960).
20. P. G. Klemens, "Lattice Thermal Conductivity," *Solid State Physics*, Vol. 7, Academic Press, New York (1957).
21. P. G. Klemens, *Phys. Rev.*, **119**, 507 (1960).
22. A. V. Ioffe and A. F. Ioffe, *Izv. Akad. Nauk. SSSR Ser Fig.*, **20**, 55 (1956).
23. R. Simon, "Maximum Figure of Merit of Thermoelectric Materials," Symposium on Thermoelectric Power Conversion, Dallas, Texas (January 1961). Paper obtained from Battelle Memorial Institute, Columbus, Ohio.